

Quantum-Chemical Calculations and IR Spectra of the  $(F_2)MF_2$  Molecules ( $M = B, Al, Ga, In, Tl$ ) in Solid Matrices: A New Class of Very High Electron Affinity Neutral MoleculesXuefeng Wang<sup>†,‡</sup> and Lester Andrews<sup>\*,‡</sup><sup>†</sup>Department of Chemistry, Tongji University, Shanghai 200092, China<sup>‡</sup>Department of Chemistry, University of Virginia, Charlottesville, Virginia 22904-4319, United States

S Supporting Information

**ABSTRACT:** Electron-deficient group 13 metals react with  $F_2$  to give the compounds  $MF_2$  ( $M = B, Al, Ga, In, Tl$ ), which combine with  $F_2$  to form a new class of very high electron affinity neutral molecules,  $(F_2)MF_2$ , in solid argon and neon. These  $(F_2)MF_2$  fluorine metal difluoride molecules were identified through matrix IR spectra containing new antisymmetric and symmetric  $M-F$  stretching modes. The assignments were confirmed through close comparisons with frequency calculations using DFT methods, which were calibrated against the  $MF_3$  molecules observed in all of the spectra. Electron affinities calculated at the CCSD(T) level fall between 7.0 and 7.8 eV, which are in the range of the highest known electron affinities.

High-oxidation-state metal fluorides are known to be very strong agents for oxidation. For example, the metal hexafluoride  $PtF_6$  can oxidize xenon to form xenon-containing compounds, as first reported by Bartlett.<sup>1</sup> The electron affinity for  $PtF_6$ , which is a direct measure of oxidizing strength, has been calculated<sup>2</sup> and measured<sup>3</sup> to be  $\sim 7$  eV, which is the highest electron affinity measured for a neutral molecule to date. The high-electron-affinity transition-metal hexafluorides from mild ( $WF_6$ ) up to extreme ( $PtF_6$ ) oxidizing strength have been extensively investigated.<sup>4</sup> However, metal fluorides with such high electron affinities have not been obtained for the main-group metals. We report here the first IR spectra of a new class of neutral  $(F_2)MF_2$  molecules ( $M = B, Al, Ga, In, Tl$ ), which exhibit high-frequency  $M-F$  stretching modes for the shorter  $M-F$  bonds and low-frequency calculated  $M-F$  modes for longer  $M-F$  bonds. The most pronounced chemical property for these group 13 fluorine metal difluoride molecules is high electron affinity (7.0–7.8 eV) based on CCSD(T) calculations, which predict very high oxidizing strengths. These new electron-deficient “ $MF_4$ ” molecules and their structures follow those for the  $BH_4$  free radical, which was recently characterized in similar experiments with B atoms and  $H_2$  molecules.<sup>5a</sup>

Laser-ablated group 13 metal atoms were reacted with  $F_2$  in excess argon and neon during condensation at 5 K using a Sumitomo Heavy Industries RDK-205D cryocooler and methods described previously.<sup>5</sup> Commercial fluorine (Air Products and Chemicals, Inc.) was used as received after storage over NaF to remove HF. Natural isotopic boron  $^{10}B$  (Aldrich, 80.4%  $^{10}B$ , 19.6%  $^{11}B$ ) and enriched  $^{10}B$  (Eagle-Picher, 93.8%  $^{10}B$ , 6.2%  $^{11}B$ ), Al (Johnson Matthey, 99.998%), Ga (Johnson Matthey), In (Indium Corporation), and Tl (Spex Industries, 99.999%) were also employed, respectively, as targets for laser

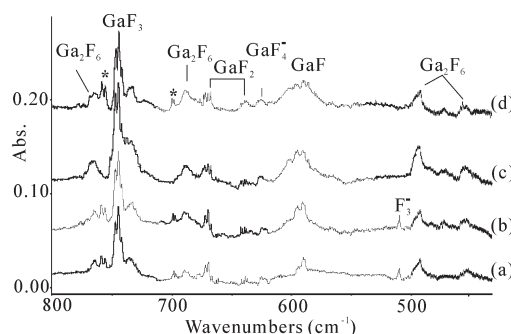


**Figure 1.** IR spectra in the product absorption region (800–430  $cm^{-1}$ ) for reactions of laser-ablated Ga atoms with  $F_2$  in excess argon at 5 K: (a) Ga + 1.5%  $F_2$  in Ar codeposited for 1 h; (b) after annealing to 20 K; (c) after  $>220$  nm irradiation; (d) after annealing to 35 K. \* labels denote the new  $(F_2)GaF_2$  absorptions.

ablation using 10–40 mJ of 1064 nm laser energy per 10 ns pulse. IR spectra were recorded, and then the samples were annealed and irradiated using a 175 W mercury arc lamp, after which more spectra were recorded. Complementary electronic structure calculations were carried out using the Gaussian 09 package,<sup>6</sup> the B3LYP density functional,<sup>7,8</sup> and coupled-cluster methods including triple excitations [CCSD(T)]<sup>9</sup> at the B3LYP minima. In DFT calculations, the aug-cc-pVTZ basis set was used for F, B, Al, and Ga and the Stuttgart ECPS and aug-cc-pVTZ-PP basis set<sup>10</sup> (21 valence electrons) for In and Tl in order to provide a consistent set of vibrational frequencies for the reaction products. Geometries were fully relaxed during optimization, and the optimized geometry was confirmed by vibrational analysis. For CCSD(T) single-point energy calculations, the aug-cc-pVTZ basis set was used for F, B, Al, and Ga and the Stuttgart ECPS and aug-cc-pVTZ-PP basis set<sup>10</sup> for In and Tl.

Typical IR spectra of the products of reactions of Ga atoms with  $F_2$  in excess argon are illustrated in Figure 1. The strongest new band systems at 748 and 592  $cm^{-1}$  were observed previously and identified as  $GaF_3$  and  $GaF$ , and we agree with these assignments.<sup>11</sup> The photosensitive band at 510  $cm^{-1}$  was recently assigned to the isolated  $F_3^-$  anion in solid argon.<sup>12</sup> Our frequency calculations show that the structured band systems at 670 and 640  $cm^{-1}$  are due to  $GaF_2$ , the band at 626  $cm^{-1}$  arises from the very stable  $GaF_4^-$  anion, and the broad bands at 766, 689, 492, and 451  $cm^{-1}$ , which increase steadily upon photolysis and annealing, are due to  $Ga_2F_6$ . The structured band patterns arise from matrix-site and gallium isotopic

Received: December 20, 2010

Published: February 25, 2011

**Table 1.** Observed and Calculated M–F Stretching Frequencies, Reaction Energies, and Geometrical Parameters for (F<sub>2</sub>)MF<sub>2</sub> Molecules (M = B, Al, Ga, In, Tl)<sup>a</sup>

vib. mode	frequencies														
	obs.			obs.			obs.			obs.			obs.		
	Ar <sup>b</sup>	Ne	calc.	Ar <sup>c</sup>	Ne	calc.	Ar	Ne	calc.	Ar	Ne	calc.	Ar	Ne	calc.
	(F <sub>2</sub> ) <sup>11</sup> BF <sub>2</sub>			(F <sub>2</sub> )AlF <sub>2</sub>			(F <sub>2</sub> ) <sup>69</sup> GaF <sub>2</sub>			(F <sub>2</sub> )InF <sub>2</sub>			(F <sub>2</sub> )TlF <sub>2</sub>		
M–F str	1389.9	1396.8	1397 (403)	931.7	945.8	939 (184)	759.1	769.0	746.2 (105)	643.5	655.7	634 (92)	618	624	602 (81)
M–F str		1161.2	1130 (362)		832.1	831 (159)	700.2	710.2	683.4 (56)	607.4	615.7	592 (33)	n.o.	n.o.	544 (11)
M–F' str			739 (41)			605 (12)			555.4 (31)			490 (33)			443 (30)
M–F' str			520 (13)			453 (0)			352.5 (7)			310 (5)			294 (31)
F'–F' str			512 (17)			350 (25)			318.9 (22)			309 (23)			256 (4)
	(F <sub>2</sub> ) <sup>10</sup> BF <sub>2</sub>						(F <sub>2</sub> ) <sup>71</sup> GaF <sub>2</sub>								
M–F str	1438.1	1445.4	1449 (437)				755.9	766.1	743.1 (103)						
M–F str		1188.6	1166 (402)				699.0	708.7	682.0 (54)						
M–F' str			743 (38)						554.4 (32)						
M–F' str			534 (13)						352.2 (6)						
electron affinities, reaction energies, and geometrical parameters															
EA <sup>d</sup>	171 (7.4)			180 (7.8)			177 (7.7)			171 (7.4)			162 (7.0)		
ΔE(M + F <sub>2</sub> ) <sup>e</sup>	–252			–225			–183			–154			–118		
ΔE(MF <sub>2</sub> + F <sub>2</sub> ) <sup>f</sup>	–124			–128			–102			–80			–49		
ΔE(MF <sub>3</sub> + F) <sup>g</sup>	11			–11			–10			–10			–9		
geom. param. <sup>h</sup>	B–F, 1.326; B–F', 1.500;			Al–F, 1.644; Al–F', 1.779;			Ga–F, 1.732; Ga–F', 1.888;			In–F, 1.934; In–F', 2.103;			Tl–F, 1.984; Tl–F', 2.224;		
	F'–F', 1.930; F–B–F, 119.8			F'–F', 2.011; F–Al–F, 121.3			F'–F', 2.017; F–Ga–F, 123.8			F'–F', 2.018; F–In–F, 128.2			F'–F', 2.010; F–Tl–F, 147.5		

<sup>a</sup> Frequencies in cm<sup>–1</sup>. Frequencies and intensities (in km/mol; values given in parentheses) were computed with the B3LYP functional and are for harmonic calculations. ⟨S(S + 1)⟩ values ranged from 0.755 to 0.758 before annihilation. <sup>b</sup> Data from ref 22. <sup>c</sup> Data from ref 19. <sup>d</sup> Electron affinities (kcal/mol) for (F<sub>2</sub>)MF<sub>2</sub> computed with CCSD(T) single-point energy; the values in parentheses are in eV. <sup>e</sup> Energy changes (kcal/mol) for the reaction M – F<sub>2</sub> → MF<sub>2</sub> computed with CCSD(T) single-point energy. <sup>f</sup> Energy changes (kcal/mol) for the reaction MF<sub>2</sub> + F<sub>2</sub> → (F<sub>2</sub>)MF<sub>2</sub> computed with CCSD(T) single-point energy. <sup>g</sup> Energy changes (kcal/mol) for the reaction MF<sub>3</sub> + F → (F<sub>2</sub>)MF<sub>2</sub> computed with CCSD(T) single-point energy. Hence, (F<sub>2</sub>)BF<sub>2</sub> is metastable, but the other (F<sub>2</sub>)MF<sub>2</sub> are stable. <sup>h</sup> Geometry parameters (distances in Å, angles in deg) calculated with B3LYP.

<sup>a</sup> Frequencies in cm<sup>–1</sup>. Frequencies and intensities (in km/mol; values given in parentheses) were computed with the B3LYP functional and are for harmonic calculations. <sup>b</sup>  $\langle S(S+1) \rangle$  values ranged from 0.755 to 0.758 before annihilation. <sup>c</sup> Data from ref 22. <sup>d</sup> Electron affinities (kcal/mol) for (F<sub>2</sub>)MF<sub>2</sub> computed with CCSD(T) single-point energy; the values in parentheses are in eV. <sup>e</sup> Energy changes (kcal/mol) for the reaction M + F<sub>2</sub> → MF<sub>2</sub> computed with CCSD(T) single-point energy. <sup>f</sup> Energy changes (kcal/mol) for the reaction MF<sub>2</sub> + F<sub>2</sub> → (F<sub>2</sub>)MF<sub>2</sub> computed with CCSD(T) single-point energy. <sup>g</sup> Energy changes (kcal/mol) for the reaction MF<sub>3</sub> + F → (F<sub>2</sub>)MF<sub>2</sub> computed with CCSD(T) single-point energy. Hence, (F<sub>2</sub>)BF<sub>2</sub> is metastable, but the other (F<sub>2</sub>)MF<sub>2</sub> are stable. <sup>h</sup> Geometry parameters (distances in Å, angles in deg) calculated with B3LYP.

splittings.<sup>13</sup> These observed frequencies are compared with calculated frequencies in Table 1. New gallium isotopic doublet bands (<sup>69</sup>Ga and <sup>71</sup>Ga, 60.1 and 39.9%, respectively, in natural abundance) were resolved at 759.1 and 755.9 cm<sup>–1</sup> and partially resolved at 700.2 and 699.0 cm<sup>–1</sup> on deposition. These bands (labeled with \* in the figures) tracked together in that they increased by 20% upon annealing to 20 K, disappeared upon 240–380 nm irradiation, recovered by 50% upon annealing to 30 K, disappeared again upon >220 nm irradiation, and recovered by 150% upon annealing to 35 K.

The neon matrix spectra shown in Figure 2 contain counterpart bands at higher frequencies with better resolved gallium isotopic splittings. The 759 and 610 cm<sup>–1</sup> bands are due to GaF<sub>3</sub> and GaF,<sup>11</sup> and the site splittings at 759.7 and 758.8 cm<sup>–1</sup> for <sup>69</sup>GaF<sub>3</sub> and at 756.7 and 755.5 cm<sup>–1</sup> for <sup>71</sup>GaF<sub>3</sub>, respectively, are clear. Isotopic doublets were also observed at 683.9, 681.3 cm<sup>–1</sup> and at 652.8, 651.5 cm<sup>–1</sup> for the two modes of GaF<sub>2</sub> and lower at 632.3, 630.1 cm<sup>–1</sup> for GaF<sub>4</sub><sup>–</sup>; bands at 779, 696, 498, and 456 cm<sup>–1</sup> for Ga<sub>2</sub>F<sub>6</sub> were seen as well. Also, a photosensitive band at 525 cm<sup>–1</sup> was recently assigned to the isolated F<sub>3</sub><sup>–</sup> anion in solid neon.<sup>12</sup> Gallium isotopic doublets were observed for the new product at 769.0 and 766.1 cm<sup>–1</sup> and at 710.2 and 708.7 cm<sup>–1</sup>. Irradiation at >380 nm decreased the new bands, while 240–380 nm irradiation destroyed them along with the F<sub>3</sub><sup>–</sup> band and increased the GaF<sub>4</sub><sup>–</sup> band. A final >220 nm irradiation decreased the GaF<sub>2</sub> and increased the GaF<sub>3</sub> and Ga<sub>2</sub>F<sub>6</sub> absorptions.

On the basis of the gallium isotopic splittings, the new product labeled \* has a single metal atom and two terminal Ga–F stretching modes, one above and one below the strong terminal Ga–F stretching modes of Ga<sub>2</sub>F<sub>6</sub> and the antisymmetric stretching mode of GaF<sub>3</sub> and both above the two stretching modes of GaF<sub>2</sub>. Thus, we appear to have made a new Ga(III) species, and (F<sub>2</sub>)GaF<sub>2</sub>, an analogue of the electron-deficient BH<sub>4</sub> free radical,<sup>5a</sup> comes to mind.

B3LYP calculations were performed for this species, and the two terminal Ga–F stretching modes were calculated to be 9 cm<sup>–1</sup> below and 11 cm<sup>–1</sup> above the two modes for Ga<sub>2</sub>F<sub>6</sub>, 11 cm<sup>–1</sup> above and 53 cm<sup>–1</sup> below that for GaF<sub>3</sub>, and above both stretching modes for GaF<sub>2</sub>, which were very nearly the same as observed (see Table S1). Furthermore the gallium isotopic splittings for the two bands calculated as 746.2 and 683.4 cm<sup>–1</sup>, which underestimate the argon matrix bands by 1.8 and 2.7%, respectively, were 3.1 and 1.4 cm<sup>–1</sup>. These values compare favorably with the 2.9 and 1.5 cm<sup>–1</sup> and 3.2 and 1.2 cm<sup>–1</sup> splittings observed in solid neon and argon, respectively. Finally, comparisons can be made to Ga<sub>2</sub>F<sub>6</sub>, which also has electron-deficient bonding. The antisymmetric terminal GaF<sub>2</sub> mode was calculated to be 755 cm<sup>–1</sup> and observed to be 766 cm<sup>–1</sup> in solid argon, and the symmetric terminal GaF<sub>2</sub> mode was calculated to be 672 cm<sup>–1</sup> and observed to be 689 cm<sup>–1</sup>; these bear almost the same relationship as the above bands calculated and observed for (F<sub>2</sub>)GaF<sub>2</sub>.

Although B3LYP-computed frequencies are typically slightly higher than the observed values,<sup>16</sup> this is not the case for the Ga–F stretching frequencies. For reference, the B3LYP frequency of 600 cm<sup>–1</sup> for GaF is 1.3% above the argon and 1.6% below the neon matrix values, and the B3LYP frequency of 736 cm<sup>–1</sup> for GaF<sub>3</sub> is 1.6% below the argon and 3.0% below the neon matrix observations. Hence, the B3LYP values for (F<sub>2</sub>)GaF<sub>2</sub> are 1.7 and 2.4% below the argon matrix and 3.0 and 3.7% below the neon matrix observations, which demonstrates similar, very good agreement between calculated and observed frequencies for the new (F<sub>2</sub>)GaF<sub>2</sub> molecule and substantiates our assignments. Unfortunately, other modes of the new (F<sub>2</sub>)GaF<sub>2</sub> molecule were too weak to be observed with the low yield of new product.

This new species is clearly photosensitive, as it was destroyed along with F<sub>3</sub><sup>–</sup> in favor of GaF<sub>4</sub><sup>–</sup> and GaF<sub>3</sub> upon 240–380 nm

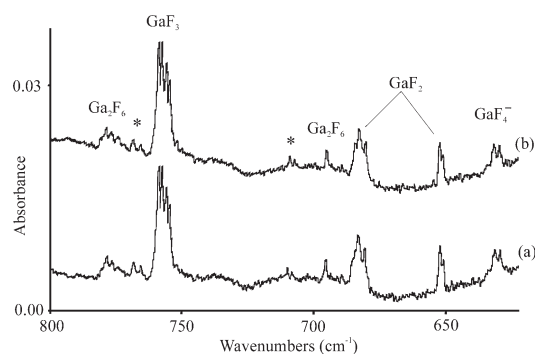
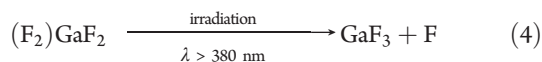


**Figure 2.** IR spectra in the product absorption region (800–620 cm<sup>-1</sup>) for reactions of laser-ablated Ga atoms with F<sub>2</sub> in excess neon at 5 K: (a) Ga + 0.5% F<sub>2</sub> in Ne codeposited for 40 min; (b) after annealing to 8 K. \* labels denote the new (F<sub>2</sub>)GaF<sub>2</sub> absorptions.

irradiation. However, it was regenerated by annealing to 30 and 35 K in solid argon, where both F atoms and F<sub>2</sub> molecules can diffuse and react with GaF<sub>3</sub> and GaF<sub>2</sub>. We observed no metal oxide bands but did see growth of the weak 1489 cm<sup>-1</sup> OOF band<sup>14</sup> upon annealing to 35 K due to the reaction with a trace O<sub>2</sub> impurity in the commercial fluorine. A straightforward explanation of this behavior includes electron photodetachment<sup>12</sup> from F<sub>3</sub><sup>-</sup> and capture by (F<sub>2</sub>)GaF<sub>2</sub> to form the very stable GaF<sub>4</sub><sup>-</sup> anion (reaction 1), which is exothermic by 177 kcal/mol [Table 1, CCSD(T)] and defines the electron affinity of (F<sub>2</sub>)GaF<sub>2</sub>. The GaF<sub>4</sub><sup>-</sup> anion absorption increases slightly on UV photolysis. Furthermore the reaction of Ga and F<sub>2</sub> (reaction 2) is exothermic by 183 kcal/mol, indicating a Ga–F bond strength of ~92 kcal/mol, and the further reaction of GaF<sub>2</sub> with F<sub>2</sub> (eq 3) is exothermic by 102 kcal/mol, characterizing the electron-deficient three-center bonding of F<sub>2</sub> to GaF<sub>2</sub>. The large energy for reaction 3 demonstrates that this new X–GaF<sub>2</sub> product is not a simple complex of GaF<sub>2</sub> with another molecule. For example, calculations find the NN–GaF<sub>2</sub> complex to be repulsive. In addition, the photosensitive nature of (F<sub>2</sub>)GaF<sub>2</sub> with >380 nm radiation in neon, which does not affect F<sub>3</sub><sup>-</sup>, is probably due to dissociation of the side-bound F<sub>2</sub> molecule (reaction 4), as fluorine itself has a continuous absorption from the UV extending out to the visible region.<sup>15</sup> Decomposition reaction 4 was calculated to be endothermic (Table 1), which indicates that (F<sub>2</sub>)GaF<sub>2</sub> is stable.



Additional support for the above chemical, photochemical, and calculational identification of (F<sub>2</sub>)GaF<sub>2</sub> was provided by the observation of the analogous group 13 (F<sub>2</sub>)MF<sub>2</sub> molecules in similar experiments. Spectra for these molecules in solid neon are compared in Figure 3. The observed and calculated M–F stretching frequencies for the (F<sub>2</sub>)MF<sub>2</sub> molecules are listed in Table 1. All of the (F<sub>2</sub>)MF<sub>2</sub> species are photoactive upon full-arc irradiation: the new B and Al counterparts increase, while the Ga, In, and Tl derivatives decrease.

The major intermediate species in the BF<sub>3</sub> system were produced by Jacox and Thompson using neon discharge irradiation.<sup>17</sup> However, the reaction of <sup>11</sup>B with F<sub>2</sub> in solid neon gave major new bands at 1396.8 and 1161.2 cm<sup>-1</sup>, which shifted to 1445.4 and 1188.6 cm<sup>-1</sup>, respectively, with <sup>10</sup>B. These bands define the same <sup>10</sup>B/<sup>11</sup>B ratio as observed for BF<sub>2</sub> but are located slightly higher than the

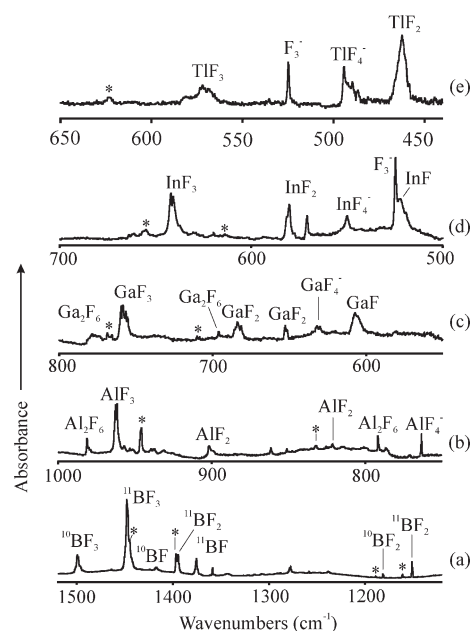


**Figure 3.** IR spectra in the product absorption regions for reactions of laser-ablated B, Al, Ga, In, and Tl atoms with F<sub>2</sub> in excess neon at 5 K: (a) <sup>11</sup>B + 0.5% F<sub>2</sub> in Ne codeposited for 1 h; (b) Al + 0.5% F<sub>2</sub> in Ne codeposited for 1 h; (c) Ga + 1% F<sub>2</sub> in Ne codeposited for 1 h; (d) In + 1% F<sub>2</sub> in Ne codeposited for 1 h; (e) Tl + 0.7% F<sub>2</sub> in Ne codeposited for 1 h. \* labels denote the new (F<sub>2</sub>)MF<sub>2</sub> absorptions.

antisymmetric and symmetric stretching modes of BF<sub>2</sub>. Figure 3 shows both boron isotopic absorptions in the natural isotopic experiment. The above new bands are assigned to (F<sub>2</sub>)BF<sub>2</sub>. It should be noted that these new bands were not observed in the BF<sub>3</sub> neon matrix experiments, although a 1397.0 cm<sup>-1</sup> shoulder was observed on the very strong 1394.0 cm<sup>-1</sup> absorption of <sup>11</sup>BF<sub>2</sub>.<sup>17</sup> In the case of Al, a strong antisymmetric Al–F stretching band was observed for AlF<sub>3</sub> at 962.5 and 961.5 cm<sup>-1</sup>, in good agreement with Snelson.<sup>18</sup> Another sharp band at 945.8 cm<sup>-1</sup> and a weak band at 832.1 cm<sup>-1</sup> were observed in solid neon and are appropriate for (F<sub>2</sub>)AlF<sub>2</sub> on the basis of the calculated values of 939 and 831 cm<sup>-1</sup> (Table 1). For reference, our B3LYP-calculated value for AlF<sub>3</sub>, 941 cm<sup>-1</sup>, is just below the matrix-observed value. Argon matrix experiments located a 931.7 cm<sup>-1</sup> band below the 947.0 cm<sup>-1</sup> band for AlF<sub>3</sub>, and although these lower bands were first thought to be matrix sites of AlF<sub>3</sub>, they are better assigned now to (F<sub>2</sub>)AlF<sub>2</sub>.<sup>18,19</sup>

Indium followed the trend for gallium in that two new bands at 655.7 and 615.7 cm<sup>-1</sup> tracked together and bracketed the 642 cm<sup>-1</sup> band for InF<sub>3</sub>, which was computed to be 615 cm<sup>-1</sup> using B3LYP. Our calculations predicted the two terminal modes for (F<sub>2</sub>)InF<sub>2</sub> to appear at 634 and 592 cm<sup>-1</sup>, which compare favorably with the observed band positions. Argon matrix counterparts were observed for (F<sub>2</sub>)InF<sub>2</sub> at 643.5 and 607.4 cm<sup>-1</sup>. For Tl, one new Tl–F stretching mode was found at 618 cm<sup>-1</sup> in solid argon and at 624 cm<sup>-1</sup> in solid neon, and these frequencies are located higher than the Tl–F stretching modes observed here for TlF<sub>3</sub> in solid argon (558 cm<sup>-1</sup>) and solid neon (570 cm<sup>-1</sup>), which was computed to be 542 cm<sup>-1</sup> using B3LYP. The bands of the new Tl product fall similarly above the calculated intense 602 cm<sup>-1</sup> mode for (F<sub>2</sub>)TlF<sub>2</sub> (Table 1). To summarize, the observation of the strongest IR absorptions for all five group 13 (F<sub>2</sub>)MF<sub>2</sub> molecules, in excellent agreement with calculations calibrated against the MF<sub>3</sub> frequencies, confirms our assignments of these new very high electron affinity molecules.



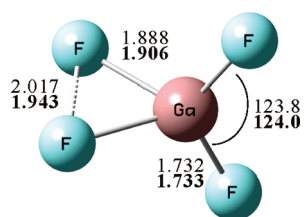


**Figure 4.** Calculated structure of  $(F_2)GaF_2$ . B3LYP values using the aug-cc-pVTZ basis set for F and Ga are in normal type, and CCSD(T) values using the 6-311+G(3df) basis set for F and the SDD (large core) set for Ga are in bold type.

The observation of the Tl(III) molecule  $TlF_3$  is important in its own right. Although the decreasing stability of trivalent fluorides from B to Tl is well-known, quadratic configuration-interaction calculations of the  $TlF_3 \rightarrow TlF + F_2$  reaction energy predicted stability for the  $TlF_3$  molecule.<sup>20</sup>

The interesting group 13 chemistry trend here should be noted: the observed antisymmetric and symmetric modes for  $(F_2)BF_2$  are just a little higher than the same modes for  $BF_2$  but much lower than the antisymmetric B–F mode for  $BF_3$ . However, for the heavier metals, the terminal M–F modes for  $(F_2)MF_2$  increase relative to that for the  $MF_3$  molecule. Finally, the strong mode for  $(F_2)TlF_2$  is located at a higher wavenumber than the antisymmetric Tl–F mode for  $TlF_3$ , suggesting the participation of electron-occupied d orbitals for Tl in charge transfer, which allows the Tl–F bonds to be more polarized. The calculated Mulliken atomic charges range from +1 for the B product to +2 for the Tl product.

Electron-deficient group 13 metals react with electron-rich  $F_2$  to give the compounds  $MF_2$ , which further combine with  $F_2$  to form the very high electron affinity neutral adduct molecules  $(F_2)MF_2$  in reactions that are exothermic by amounts ranging from 128 kcal/mol for  $AlF_2 + F_2$  to 49 kcal/mol for  $TlF_2 + F_2$  (Table 1). These  $(F_2)MF_2$  molecules are unique: the two longer M–F bonds in  $(F_2)MF_2$  include the weak  $F \cdots F$  interaction using three-electron–three-center bonds, which is substantiated by a natural bond orbital analysis of the DFT-computed molecular orbitals. The computed structure of  $(F_2)GaF_2$  is given in Figure 4. Notably, the  $F \cdots F$  bond length is near that calculated for one-electron-bonded  $F_2^-$  and the calculated  $F'-F'$  stretching frequencies (Table 1) are in the range of those measured for the alkali metal  $(M^+)(F_2^-)$  species.<sup>12,21</sup> However, this weak  $F \cdots F$  bond is cleaved upon electron attachment to give the very stable tetrahedral anion  $MF_4^-$ . The electron affinities calculated with CCSD(T) fall between 7.8 eV for  $(F_2)AlF_2$  and 7.0 eV for  $(F_2)TlF_2$  (Table 1) for this new class of very high electron affinity molecules.

## ■ ASSOCIATED CONTENT

**Supporting Information.** Complete ref 6, calculated  $GaF_x$  product frequencies and Mulliken atomic charges, and additional IR spectra. This material is available free of charge via the Internet at <http://pubs.acs.org>.

## ■ AUTHOR INFORMATION

**Corresponding Author**  
lsa@virginia.edu

## ■ ACKNOWLEDGMENT

We gratefully acknowledge financial support from NSF Grant CHE 03-52487 to L.A., NSFC Grant 20973126 to X.W., and NCSA

Computing Grant CHE07-0004N, fluorine from J. Thrasher, and helpful suggestions from D. A. Dixon.

## ■ REFERENCES

- (1) (a) Bartlett, N. *Proc. Chem. Soc.* **1962**, 218. (b) Graham, L.; Gaudejus, O.; Jha, N. K.; Bartlett, N. *Coord. Chem. Rev.* **2000**, 197, 321.
- (2) (a) Craciun, R.; Picone, D.; Long, R. T.; Li, S.; Dixon, D. A. *Inorg. Chem.* **2010**, 49, 1056. (b) Craciun, R.; Long, R. T.; Dixon, D. A.; Christe, K. O. *J. Phys. Chem. A* **2010**, 114, 7571. (c) Macgregor, S. A.; Moock, K. H. *Inorg. Chem.* **1998**, 37, 3284. (d) Wesendrup, R.; Schwerdtfeger, P. *Inorg. Chem.* **2001**, 40, 3351. (e) Riedel, S.; Kaupp, M. *Inorg. Chem.* **2006**, 45, 1228. (f) Riedel, S. *J. Fluorine Chem.* **2007**, 128, 938.
- (3) Korobov, M. V.; Kuznetsov, S. V.; Sidorov, L. N.; Shipachev, V. A.; Mit'kin, V. N. *Int. J. Mass. Spectrom. Ion Processes* **1989**, 87, 13.
- (4) For example, see: (a) Molski, M. J.; Seppelt, K. *Dalton Trans.* **2009**, 3379 and references therein. (b) Roessler, B.; Seppelt, K. *Angew. Chem., Int. Ed.* **2000**, 39, 1259. (c) Giese, S.; Seppelt, K. *Angew. Chem., Int. Ed. Engl.* **1994**, 33, 461. (d) Seidel, S.; Seppelt, K. *Angew. Chem., Int. Ed.* **2000**, 39, 3923. (e) Haiges, N. R.; Boatz, J. A.; Bau, R.; Schneider, S.; Schroer, T.; Yousufuddin, M.; Christe, K. O. *Angew. Chem., Int. Ed.* **2005**, 44, 1860. (f) Pfennig, V.; Robertson, N.; Seppelt, K. *Angew. Chem., Int. Ed. Engl.* **1997**, 36, 1350. (g) Kleinhenz, S.; Pfennig, V.; Seppelt, K. *Chem.–Eur. J.* **1998**, 4, 1687.
- (5) (a) Andrews, L.; Wang, X. *J. Am. Chem. Soc.* **2002**, 124, 7280 and references therein. (b) Wang, X.; Andrews, L.; Tam, S.; DeRose, M. E.; Fajardo, M. E. *J. Am. Chem. Soc.* **2003**, 125, 9218. (c) Andrews, L.; Wang, X. *Angew. Chem., Int. Ed.* **2004**, 43, 1706.
- (6) Frisch, M. J.; et al. *Gaussian 09*, revision A.1; Gaussian, Inc.: Wallingford, CT, 2009.
- (7) (a) Becke, A. D. *J. Chem. Phys.* **1993**, 98, 5648. (b) Lee, C.; Yang, Y.; Parr, R. G. *Phys. Rev. B* **1988**, 37, 785.
- (8) Perdew, J. P.; Burke, K.; Wang, Y. *Phys. Rev. B* **1996**, 54, 16533 and references therein.
- (9) Pople, J. A.; Head-Gordon, M.; Raghavachari, K. *J. Chem. Phys.* **1987**, 87, 5968 and references therein.
- (10) (a) Peterson, K. A. *J. Chem. Phys.* **2003**, 119, 11099. (b) Metz, B.; Schweizer, M.; Stoll, H.; Dolg, M.; Liu, W. *Theor. Chem. Acc.* **2000**, 104, 22.
- (11) Hastie, J. W.; Hauge, R. H.; Margrave, J. L. *J. Fluorine Chem.* **1974**, 3, 285.
- (12) Riedel, S.; Köchner, T.; Wang, X.; Andrews, L. *Inorg. Chem.* **2010**, 49, 7156.
- (13) (a) Burkholder, T. R.; Yustein, J. T.; Andrews, L. *J. Phys. Chem.* **1992**, 96, 10189. (b) Wang, X.; Andrews, L. *J. Phys. Chem. A* **2003**, 107, 11371.
- (14) Jacox, M. E. *Vibrational and Electronic Energy Levels of Polyatomic Transient Molecules*; J. Phys. Chem. Ref. Data Monograph 3, 1994; Jacox, M. E. *J. Phys. Chem. Ref. Data* **1998**, 27, 115; **2003**, 32, 1.
- (15) Huber, K. P.; Herzberg, G. *Constants of Diatomic Molecules*; Van Nostrand Reinhold: New York, 1979.
- (16) (a) Scott, A. P.; Radom, L. *J. Phys. Chem.* **1996**, 100, 16502. (b) Andersson, M. P.; Uvdal, P. L. *J. Phys. Chem. A* **2005**, 109, 2937. The Ga–F stretching frequencies computed using the BPW91 functional are 30  $cm^{-1}$  lower than the values obtained using B3LYP.
- (17) Jacox, M. E.; Thompson, W. E. *J. Chem. Phys.* **1995**, 102, 4747.
- (18) Snelson, A. *J. Phys. Chem.* **1967**, 71, 3202.
- (19) Hassanzadeh, P.; Citra, A.; Andrews, L.; Neurock, M. *J. Phys. Chem.* **1996**, 100, 7317.
- (20) (a) Schwerdtfeger, P.; Heath, G. A.; Dolg, M.; Bennett, M. A. *J. Am. Chem. Soc.* **1992**, 114, 7518 and references therein. (b) Schwerdtfeger, P.; Ischtwan, J. *J. Comput. Chem.* **1993**, 14, 913.
- (21) Howard, W. F., Jr.; Andrews, L. *J. Am. Chem. Soc.* **1973**, 95, 3045.
- (22) Hassanzadeh, P.; Andrews, L. *J. Phys. Chem.* **1993**, 97, 4910.